

Preparation of Activated Carbon-SnO, TiO and WO Catalysts. Study by FT-IR Spectroscopy

Adrián Barroso-Bogeat, María Alexandre-Franco, Carmen Fernández-González, Antonio Macias-Garcia, and Vicente Gomez Serrano

Ind. Eng. Chem. Res., **Just Accepted Manuscript** • DOI: 10.1021/acs.iecr.5b04563 • Publication Date (Web): 01 Feb 2016

Downloaded from <http://pubs.acs.org> on February 2, 2016

Just Accepted

“Just Accepted” manuscripts have been peer-reviewed and accepted for publication. They are posted online prior to technical editing, formatting for publication and author proofing. The American Chemical Society provides “Just Accepted” as a free service to the research community to expedite the dissemination of scientific material as soon as possible after acceptance. “Just Accepted” manuscripts appear in full in PDF format accompanied by an HTML abstract. “Just Accepted” manuscripts have been fully peer reviewed, but should not be considered the official version of record. They are accessible to all readers and citable by the Digital Object Identifier (DOI®). “Just Accepted” is an optional service offered to authors. Therefore, the “Just Accepted” Web site may not include all articles that will be published in the journal. After a manuscript is technically edited and formatted, it will be removed from the “Just Accepted” Web site and published as an ASAP article. Note that technical editing may introduce minor changes to the manuscript text and/or graphics which could affect content, and all legal disclaimers and ethical guidelines that apply to the journal pertain. ACS cannot be held responsible for errors or consequences arising from the use of information contained in these “Just Accepted” manuscripts.

1 Preparation of Activated Carbon-SnO₂, TiO₂ and WO₃

2 Catalysts. Study by FT-IR Spectroscopy

3 Adrián Barroso-Bogeat,[†] María Alexandre-Franco,[†] Carmen Fernández-González,[†]
4 Antonio Macías-García,[‡] Vicente Gómez-Serrano^{*,†}

5 [†]Department of Organic and Inorganic Chemistry, Faculty of Sciences, University of Extremadura, 06006 Badajoz, Spain

6 [‡]Department of Mechanical Engineering, Energetic and of Materials, School of Industrial Engineering, University of Extremadura,
7 06006 Badajoz, Spain

8

9 **ABSTRACT:** The chemical changes produced in the surface of activated carbon as a
10 result of the process of preparation of activated carbon-metal oxide catalysts from
11 SnCl₂, TiO₂ and Na₂WO₄ in water at pH 1.37 for SnCl₂, 5.84 for TiO₂ and 9.54 for
12 Na₂WO₄ are studied. The samples were first prepared by the wet impregnation method
13 in two successive steps of soaking at 80 °C for 5 h and oven-drying at 120 °C for 24 h.
14 Then, they were analyzed by elemental analysis, FT-IR spectroscopy and measurement
15 of pH of the point of zero charge (pH_{pzc}). The process yield was 149 wt% with SnCl₂,
16 102 wt% with TiO₂ and 106 wt% with Na₂WO₄. The impregnation of the carbon with
17 the catalyst precursors in water entails the oxidation of chromene and pyrone type
18 structures with formation of carboxylic acid groups. pH_{pzc} is: 10.50, activated carbon; <
19 1.60, SnCl₂; 9.35, TiO₂; and 7.90, Na₂WO₄. The changes originated in the surface
20 chemistry of AC with influence on the acid-base character are stronger by the order
21 SnCl₂ >> Na₂WO₄ > TiO₂.

22

23

24 ■ INTRODUCTION

25 In heterogeneous catalysis, activated carbon (AC) is used as catalyst and mainly as a
26 support for catalysts. As a support, high-surface-area microporous ACs are the most
27 commonly used materials as very high catalyst dispersions can be achieved easily, thus
28 resulting in high catalytic activity.^{1,2} An additional virtue of ACs is the combined effect
29 of molecular sieving, similar to that of zeolite.¹ Furthermore, they are resistant to acidic
30 and basic media.³ However, it has also been stated that carbon as a support material is
31 much less inert than assumed by the catalysis community.¹ In many cases, the role of
32 the carbon support is not restricted to providing a large surface on which the sintering of
33 the active catalytic species will be minimized. In the catalyst preparation the interaction
34 between the liquid catalyst precursor and the carbon surface is crucial and often
35 misunderstood.¹ That is why new insights into the chemical changes produced on AC's
36 surface because of the process of preparation of the catalyst support are needed with a
37 view to tailoring the catalyst composition to benefit its activity in catalysis processes
38 and also for regeneration purposes. Metal oxide (MO) catalysts such as SnO₂, TiO₂ and
39 WO₃ supported on AC have been used for a great variety of chemical reactions.⁴ In
40 recent years, TiO₂/AC photo-catalysts in particular have drawn vast interest due to its
41 potential to degrade organic micro-pollutants in water.⁵⁻²⁰ Herein, the chemical changes
42 produced in the surface of AC and in its acid-base character as a result of the
43 preparation of the AC-MO samples from SnCl₂, TiO₂ and WO₄²⁻ in water by the wet
44 impregnation method are studied by means of FT-IR spectroscopy and also by
45 measuring pH of the point of zero charge. Data of the elemental composition for the
46 samples are also reported.

47

48 ■ MATERIALS AND METHODS

49 **Materials and reagents.** In the preparation of the AC-MO samples, a granular
50 AC (Merck; Darmstadt, Germany, Cod. 1.02514.1000; 1.5 mm average particle size)
51 and $\text{SnCl}_2 \cdot 2\text{H}_2\text{O}$ and $\text{Na}_2\text{WO}_4 \cdot 2\text{H}_2\text{O}$ (Panreac; Barcelona, Spain; reagent grade) and
52 anatase powder (Aldrich; Steinheim, Germany; particle size lower than 44 μm) were
53 used. The starting AC was previously studied from the standpoint of surface functional
54 groups and structures.²¹ Also, the AC-MO samples were characterized in terms of
55 porous structure and chemical composition.^{22,23} The impregnation solutions were
56 prepared from deionized water at pH 5.05. The pH of the impregnation solutions is
57 listed in Table 1. Such solutions were used immediately after preparation, without
58 previous deaeration.

59 **Preparation of the samples.** The preparation of the AC-MO samples was
60 carried out by the wet impregnation method in two successive steps of soaking at 80 °C
61 for 5 h and oven-drying at 120 °C for 24 h, as described in detail elsewhere.^{22,23} In the
62 case of TiO_2 , however, a slightly modified impregnation method at high temperature
63 previously proposed by Kahn and Mazyck was used.^{24,25} In such a method, 25 g of AC
64 were impregnated with 250 mL of an aqueous suspension containing 1.25 g of anatase
65 powder and the resulting mixture was also heated at 80 °C for 5 h under stirring of 300
66 rpm. After vacuum-filtration, the resulting solid in two successive steps was thoroughly
67 washed with deionised water until total colour loss in the residual liquid and oven-dried
68 at 120 °C for 24 h. Anatase was selected as the catalyst precursor because the
69 photocatalytic activity of TiO_2 seems to be mainly associated with the anatase-type
70 structure.²⁶ The yield of the process of preparation of the samples was estimated by the
71 following expression:

1
2
3
4
5
6
7
8
9
10
11
12
13
14
15
16
17
18
19
20
21
22
23
24
25
26
27
28
29
30
31
32
33
34
35
36
37
38
39
40
41
42
43
44
45
46
47
48
49
50
51
52
53
54
55
56
57
58
59
60

$$72 \quad Y(\%) = \frac{M_f(g)}{M_i(g)} \cdot 100 \quad (1)$$

73 where M_i is the initial mass of AC and M_f is the final mass of AC-MO sample. The
74 yield values are given in Table 1, together with sample codes.

75 **Analysis of the samples.** The elemental analysis of the samples (C, H, N and S)
76 was performed in an analyzer (CHNS-932, LECO), whereas the O content was
77 estimated by difference. In addition, the samples were analyzed by FT-IR spectroscopy,
78 using a Perkin Elmer Spectrum 100 spectrometer. Spectra were recorded in the range of
79 wave numbers from 4000 to 400 cm^{-1} , using sample/KBr pellets prepared as described
80 elsewhere.²¹ pH of the point zero charge (pH_{pzc}) was determined following the method
81 previously proposed by Newcombe et al.^{27,28} 0.01 M NaCl aqueous solutions at pH 2, 4,
82 6, 8 and 10 were prepared by fixing these pH values with either 0.1 M HCl or NaOH
83 aqueous solution. The pH_{pzc} was obtained from the plot of pH of the initial solution
84 against pH of the corresponding supernatant.

85

86 ■ RESULTS AND DISCUSSION

87 **Solution/suspension pH.** The pH of the impregnation solution (see Table 1) was
88 1.37 for SnCl_2 , 5.84 for TiO_2 and 9.54 for WO_4^{2-} . As regard SnCl_2 , the freshly prepared
89 aqueous solution looked cloudy with a milk-white appearance. From the low pH of the
90 SnCl_2 solution it becomes clear that in the preparation of this solution chemical changes
91 occurred in SnCl_2 after contact with water. Stannous chloride is readily soluble in water,
92 its solubility being as high as 178 g SnCl_2 per 100 g water at 10 °C.²⁹ The chemical
93 behavior of SnCl_2 in excess water depends on a number of factors including solution
94 pH, concentration, storage time, and presence of aerial oxygen.³⁰⁻³⁵ Among other

1
2
3 95 processes, SnCl_2 undergoes hydrolysis and oxidation with formation of HCl which
4
5 96 accounts for the great pH decrease for the SnCl_2 solution. Titanium dioxide in water
6
7 97 must be hydroxylated. In fact, the TiO_2 surface is known to be readily covered with
8
9 98 hydroxyl groups in a water-reach environment,³⁶ as TiO_2 has both Lewis acidic and
10
11 99 basic centers which allow its surface to be easily hydroxylated by dissociative and
12
13 100 molecular water adsorption.³⁷ The pH of 9.54 for the $\text{Na}_2\text{WO}_4 \cdot 2\text{H}_2\text{O}$ solution falls
14
15 101 within the pH range 9.15-10.5 reported in the literature for molar solutions prepared
16
17 102 from $\text{Na}_2\text{WO}_4 \cdot 2\text{H}_2\text{O}$ and purified water.³⁸ The alkalinity of the WO_4^{2-} solution may be
18
19 103 due to the presence of excess alkali (i.e. NaOH) in commercial $\text{Na}_2\text{WO}_4 \cdot 2\text{H}_2\text{O}$ or to the
20
21 104 hydrolysis and polymerization of Na_2WO_4 .³⁸

22
23
24
25
26 105 **Process yield.** As shown in Table 1, the yield of the process of preparation of
27
28 106 the samples was 149 wt% for S120, 103 wt% for T120 and 106 wt% for W120, and
29
30 107 therefore strongly dependent on the nature of the chemical species used in the
31
32 108 impregnation of AC. Probably, a major factor influencing the process yield was the
33
34 109 exiting speciation in the impregnation solution as it should control mass transport in
35
36 110 pores of the carbon and thereby the amount of catalyst precursor ultimately loaded on
37
38 111 AC. First, the very high yield for S120 is compatible with a facilitated diffusion of small
39
40 112 size tin species in the accessible porosity of AC. Perhaps, as the impregnation of AC
41
42 113 with the aforesaid SnCl_2 solution was carried out immediately after preparation, large
43
44 114 tin polynuclear and polymerized species were formed only to a reduced extent.
45
46 115 Likewise, the proportion and size of colloidal particles should be small in the freshly
47
48 116 prepared SnCl_2 solution. In fact, as reported elsewhere,³³ colloids are composed of tin
49
50 117 species such as SnO_2 and Sn_3O_4 . Furthermore, SnO_2 originates as soon as SnCl_2 is
51
52 118 brought into contact with air.³⁹ Second, the lower yield for T120 can be accounted for
53
54 119 by the large size of the TiO_2 (anatase) particles which could not enter a very important
55
56
57
58
59
60

1
2
3 120 fraction of the AC porosity as AC is mainly a microporous carbon.²² Third, the much
4
5 121 lower yield for W120 than for S120 denotes the involvement of larger size species in
6
7 122 the diffusion process for the sample prepared with WO_4^{2-} . In the presence of AC, the
8
9 123 WO_4^{2-} anion should provide the medium with an O^{2-} ion (i.e. pK_{eq} for $\text{O}^{2-} + \text{H}_2\text{O} =$
10
11 124 2OH^- being ~ -22) and this leads to the formation of WO_3 .

125 **Elemental composition.** Data of the elemental analysis (C, H, N and S; O, by
126 difference) obtained for AC, S120, T120 and W120 are listed in Table 2. As expected,
127 they show that carbon is the predominant element in AC. Oxygen is also an abundant
128 chemical constituent of AC, although much less than for carbon. However, hydrogen,
129 nitrogen and sulfur are minor heteroatoms in AC. As compared to AC, the C, N and S
130 contents are more or less lower for S120 and W120, in accordance with the process
131 yield. Conversely, the O and H contents are much higher for S120 and W120, which is
132 in line with the incorporation of oxygen as SnO_2 and WO_3 to AC and also with the trend
133 exhibited by these metal oxides to hydration, as demonstrated by the presence of two
134 water molecules in the compounds used in the preparation if the impregnation solutions
135 in the present study. In marked contrast especially to S120, the C and O contents are
136 similar for T120 and AC. However, the H content is much lower for T120 than for AC
137 and the N content is much higher for T120. From these results it becomes apparent that
138 during the preparation of T120 the incorporation of O as TiO_2 to AC was accompanied
139 with the removal of not only O but also of H, may be as H_2O .

140 **Infrared analysis.** The FT-IR spectra registered for S120, T120 and W120 are
141 shown in Figs. 1 and 2, together with the spectrum of AC which has also been plotted
142 together with the spectra for the AC-MO samples for comparison purposes. Between
143 4000 and 2000 cm^{-1} all spectra have been plotted on an expanded y-axis scale in order to

1
2
3 144 make easier their analysis. The number of features shown in the spectrum of AC were
4
5 145 tentatively ascribed elsewhere and summarized in Table 3.²¹
6
7

8 146 **Sample S120.** With respect to the spectrum of AC, in the spectrum of S120
9
10 147 (Figs. 1 and 2) a series of major changes concerning the number, position and intensity
11
12 148 of registered bands are noted in the analyzed spectral regions of 4000-2000 and 2000-
13
14 149 400 cm^{-1} . First, at frequencies above 3500 cm^{-1} , a new peak appears at 3771 cm^{-1} and
15
16 150 the intensity of the peaks at 3636, 3661 and 3701 cm^{-1} noticeably increases. These
17
18 151 features are ascribable to $\nu(\text{O-H})$ vibrations of surface hydroxyl groups present in SnO_2 .
19
20 152 As a general rule, the $\nu(\text{O-H})$ absorption frequency depends on the nature of the atom to
21
22 153 which the OH group is bonded and on the coordination of this atom within the
23
24 154 surface.^{40,41} Therefore, the absorption bands of $\nu(\text{O-H})$ vibration appearing in the S120
25
26 155 spectrum argues for surface tin atoms in different coordination states. Second, the shift
27
28 156 to higher frequencies and dissimilar shape of the bands at 2986 and 2885 cm^{-1} are also
29
30 157 worth mentioning because, according to previous band assignments,²¹ these results
31
32 158 indicate that chromene structures of AC suffered significant changes because of the
33
34 159 process of preparation of S120.
35
36
37
38
39

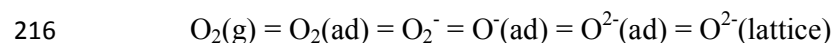
40 160 In the spectral region below 2000 cm^{-1} (Fig. 2), the great intensity increase of the
41
42 161 couple of bands at 1729 and 1286 cm^{-1} is indicative of a greatly enhanced presence of
43
44 162 carboxylic acid groups ($-\text{COOH}$) in S120. Characteristic absorptions of the carboxyl
45
46 163 group are not only at $\sim 1700 \text{ cm}^{-1}$ (vs) and 1300-1200 cm^{-1} (s) but also at $\sim 1400 \text{ cm}^{-1}$
47
48 164 (m) and $\sim 900 \text{ cm}^{-1}$ (w) due to bond stretching and deformation vibrations.⁴² Probably,-
49
50 165 COOH groups were generated from pyrone and chromene type structures of AC, as a
51
52 166 wide series of spectral features (i.e. shoulders at 1675, 1636 and 1249 cm^{-1} , etc.), which
53
54 167 were registered in the spectrum of AC and associated with the aforesaid structures, are
55
56
57
58
59
60

1
2
3 168 not visible in the spectrum of S120. In this connection a very remarkable spectral
4
5 169 change concerns the band at 1024 cm^{-1} in the spectrum of AC as this band is shifted to
6
7 170 1020 cm^{-1} and clearly shows a very pronounced absorption decrease (as a guide, see the
8
9 171 lower frequency branch from the absorption maximum down to $\sim 935 \text{ cm}^{-1}$) for S120. In
10
11 172 addition, the band at 1020 cm^{-1} is markedly weaker than the band at 1073 cm^{-1} for S120,
12
13 173 unlike for AC. Since the band at 1024 cm^{-1} was tentatively ascribed before to the
14
15 174 aforementioned reducing structures of AC,²¹ the here obtained results corroborate that
16
17 175 they were involved in the process of formation of the $-\text{COOH}$ groups during the process
18
19 176 of preparation of S120. Furthermore, a higher content of $-\text{COOH}$ groups in S120 than
20
21 177 in AC is also supported by the fact that no readily visible absorption band at around
22
23 178 1560 cm^{-1} is noted in the spectrum of S120, which is compatible with an increased
24
25 179 degree of substitution in benzene rings and consequently of symmetry gain and skeletal
26
27 180 $\text{C}=\text{C}$ vibration inactivation. Moreover, the shift of the band from 1720 cm^{-1} for AC to
28
29 181 1729 cm^{-1} for S120 argues for an increase in the content of hydrogen-bonded aliphatic $-\text{COOH}$
30
31 182 COOH groups in the case of S120.⁴³
32
33
34
35
36

37 183 A remarkable change in the spectrum of S120 is the markedly broader and
38
39 184 stronger band at 1126 cm^{-1} than the band at 1166 cm^{-1} in the spectrum of AC. To an
40
41 185 enhanced absorption at around 1126 cm^{-1} may contribute the Sn-OH group and the O_2^-
42
43 186 ion because of $\delta(\text{Sn-OH})$ and $\nu(\text{O-O})$ vibrations. In fact, the corresponding band to the
44
45 187 O_2^- ion appears in the frequency range 1180-1060 cm^{-1} .⁴⁰ Also, absorption due to the
46
47 188 $\nu(\text{C-O})$ vibration of C-O-Sn atomic groupings may take place in the spectral region of
48
49 189 1126 cm^{-1} . The medium intensity band lying at 1020 cm^{-1} is attributable to $\nu_s(\text{C-O-C})$
50
51 190 vibrations of ether type structures coming from AC,⁴⁴ which were chemically stable and
52
53 191 remained unaltered after the preparation of S120. The surface Sn-O-Sn linkages absorb
54
55 192 below 770 cm^{-1} .⁴⁵⁻⁴⁸ For crystalline and amorphous components of SnO_2 , the band
56
57
58
59
60

1
2
3 193 usually appears at 625 and 675 cm^{-1} or at 550 cm^{-1} , respectively.⁴⁹ However, in
4
5 194 connection with band assignments for SnO_2 it should be taken into account that, as
6
7 195 previously reported by Baraton,⁵⁰ the performance of infrared studies on SnO_2 surface is
8
9 196 handicapped by the instability of the material with regard to stoichiometry. As a
10
11 197 consequence of oxygen sub-stoichiometry the conductivity of the material increases,
12
13 198 leading to an opacity of the sample to IR radiation.

16
17 199 Likely, the oxidation of surface groups of AC with formation of $-\text{COOH}$ groups
18
19 200 occurred with involvement of strong oxidizing species generated as a result of the
20
21 201 oxidation to Sn(II) (i.e. metastable or dative peroxides which are characterized by a high
22
23 202 energy content and great instability)⁵¹ during the soaking step or of O_2 (air) in a reaction
24
25 203 catalyzed by SnO_2 during the oven-drying step. As is well known, many oxides mainly
26
27 204 act as a support material for dispersed metal catalysts; tin oxide, however, is an
28
29 205 oxidation catalyst in its own right. As in most oxide catalysts the oxidation reactions are
30
31 206 supposed to follow the Mars-van Krevelen mechanism. Thus, adsorbed molecules are
32
33 207 oxidized by consuming lattice oxygen of the oxide catalyst which in turn is re-oxidized
34
35 208 by gas-phase oxygen. This is possible because transition and post-transition oxides have
36
37 209 multivalent oxidation states that allow the material to easily give up lattice oxygen to
38
39 210 react with adsorbed molecules and can be subsequent re-oxidize by gas-phase oxygen.⁵²
40
41 211 As a guide, in the case of SnO_2 its surface exhibits high adsorption properties and high
42
43 212 reactivity due to the presence of free electrons in the conduction band and to the
44
45 213 presence of surface and volume oxygen vacancies and of active chemisorbed oxygen.
46
47 214 Adsorbed oxygen can be present in various chemical species according to the following
48
49 215 processes.^{53,54}



1
2
3 217 The temperature dependence of the various species was examined by Chang,⁵⁵
4
5 218 observing a transition temperature at 150 °C. Below which oxygen is mainly present as
6
7 219 O_2^- and above chemisorbed oxygen in the form of O^- or O^{2-} is present. Depending on the
8
9 220 temperature at the surface of transition metal-metal oxides there can appear ions O_2^- or
10
11 221 O^- as a result of chemisorption. Ion of O_2^- is classified as an “electrophilic” agent while
12
13 222 ions O^{2-} connected with the lattice at the surface as a “nucleophilic” agent.^{56,57}
14
15
16 223 Therefore, in the case of our reaction system, oxygen transfer should occur from SnO_2
17
18 224 to AC.
19
20

21
22 **Sample T120.** Unlike the spectrum of AC and especially of S120, the spectrum
23
24 226 of T120 between 3800 and 3600 cm^{-1} does not show features ascribable to free –OH
25
26 227 groups. In the case of T120, the –OH surface groups seem to be involved in hydrogen
27
28 228 bonding as the spectrum of this sample displays the broad band centered at 3458 cm^{-1} ,
29
30 229 which is compatible with the presence of such a physical bond in the sample.
31
32 230 Furthermore, phenolic –OH groups were detected in AC and TiO_2 has a high tendency
33
34 231 to hydroxylation,^{36,58} as commented above. At lower frequencies in the T120 spectrum,
35
36 232 the weak bands at 2980 and 2881 cm^{-1} also appear in the spectrum of AC. Notice that
37
38 233 band positions and intensities are similar in the spectra of both samples. Therefore,
39
40 234 according the here obtained FT-IR results, the – CH_2 – groups present initially in AC did
41
42 235 not undergo appreciable chemical changes after the preparation of T120. Although such
43
44 236 groups may be found in a different molecular configuration in both samples as the band
45
46 237 is shifted to slightly higher frequencies for T120.
47
48
49

50
51 238 Below 2000 cm^{-1} , the spectrum of T120 at first sight is also fairly well similarly
52
53 239 shaped to the spectrum of AC. Thus, the former spectrum displays the broad series of
54
55 240 stronger absorption bands at nearly the same frequencies (i.e. 1721, 1566, 1279, 1163,
56
57 241 1117, 1070, 1033, and 740 cm^{-1}) that are registered as well in the spectrum of AC. Also,
58
59
60

1
2
3 242 shoulders in the frequency ranges $1721\text{-}1619\text{ cm}^{-1}$ and $1279\text{-}1224\text{ cm}^{-1}$ are readily
4
5 243 visible in the spectrum of T120. Therefore, the surface groups and structures of AC
6
7 244 were largely preserved after the impregnation of AC with the TiO_2 suspension in the
8
9 245 preparation of T120, as expected because TiO_2 is a chemically stable substance.⁵⁹
10
11 246 However, the number of shoulders between 1721 and 1619 cm^{-1} and band intensities at
12
13 247 around 1721 cm^{-1} and 1033 cm^{-1} are different in both spectra. Clearly, the 1720 cm^{-1}
14
15 248 band is somewhat stronger and and the band at 1033 cm^{-1} for T120 is noticeably
16
17 249 weaker than the band at 1024 cm^{-1} for AC. From these results it is evident that C-O-C
18
19 250 containing reducing structures of AC in part, at least, were oxidized and transformed
20
21 251 into -COOH groups during the process of preparation of T120. Probably, the oxidation
22
23 252 of AC was facilitated as a result of the large particle size of TiO_2 (i.e. lower than $44\text{ }\mu\text{m}$)
24
25 253 which would not effectively prevent the oxidizing agent from entering smaller size
26
27 254 pores of AC, where most part of the surface area of microporous solids such as AC
28
29 255 concentrates, that would remain then available for oxidation during the preparation of
30
31 256 T120. Another spectral change noted in the spectrum of T120 concerns the medium
32
33 257 intensity band at 1435 cm^{-1} , which is not registered in the spectrum of S120 and that
34
35 258 may be associated with carboxylate groups formed between -COOH groups of AC and
36
37 259 TiO_2 surfaces.⁵⁸ Alternatively, such a spectral feature may be due to $\nu(\text{COO}^-)$ vibrations
38
39 260 of CO_2^- and CO_3^{2-} or HCO_3^- formed after chemisorption of carbon species on TiO_2 .⁶⁰⁻⁶²
40
41 261 On the other hand, the spectrum of T120 also displays bands and shoulders in the 800-
42
43 262 400 cm^{-1} frequency range that are ascribable to ring substitution and $\nu(\text{Ti-O})$
44
45 263 vibrations,⁶³ according to the strong band at 690 cm^{-1} with a pronounced shoulder at 545
46
47 264 cm^{-1} exhibited by the infrared spectrum obtained separately for the starting anatase used
48
49 265 in the preparation of T120, which is plotted in Fig. 3.
50
51
52
53
54
55
56
57
58
59
60

1
2
3 266 **Sample W120.** The spectrum of W120 between 4000 and 2000 cm^{-1} displays a
4
5 267 very broad band in the range 4000-3450 cm^{-1} , which is centered at 3699 cm^{-1} and that is
6
7 268 decorated with a large number of barely defined peaks. These spectral features are
8
9 269 compatible with the presence in this sample of a variety of free $-\text{OH}$ groups, the
10
11 270 contents of which being low. Also, molecular water absorbing in such a spectral region
12
13 271 may be found in W120 as hydration water of WO_3 that remained in the sample after
14
15 272 oven-drying at 120 $^\circ\text{C}$ in its preparation. It is supported by the fact that the dehydration
16
17 273 of hydrate precursors of both various metastable and stable WO_3 occurs at higher
18
19 274 temperatures in the range 235-350 $^\circ\text{C}$.⁶⁴ At lower frequencies in the region of 2900-2800
20
21 275 cm^{-1} the only noticeable spectral change is the absence from the spectrum of W120 of
22
23 276 the weak peak at 2973 cm^{-1} in the spectrum of AC. Otherwise, there must be
24
25 277 overlapping bands on account of the absorption increase produced at higher frequencies.
26
27 278 In any event, these results seem to indicate occurrence of changes in the $-\text{CH}_2-$ groups
28
29 279 of chromene type structures present in AC because of the preparation of W120.
30
31
32
33

34
35 280 The fact that the spectrum of W120 between 2000 and 400 cm^{-1} only features
36
37 281 very weak bands evidences that W120 was little amenable to the infrared analysis,
38
39 282 which must be necessarily connected with the presence of WO_3 in this sample. Because
40
41 283 tungsten is a very heavy metal, its density being as high as 19.3 g cm^{-3} ,⁶⁵ the content of
42
43 284 carbon in the weighed amount of W120 used in the preparation of the W120:KBr pellet
44
45 285 was surely low, this affecting the sensitivity of the infrared analysis. Accordingly, a
46
47 286 transmittance-axis expanded spectrum was plotted in Fig. 4. As compared to the
48
49 287 spectrum of AC, it is worth noting the increased intensity of the strong bands at 1721
50
51 288 and 1284 cm^{-1} together with the absence of shoulders at 1657 and 1636 cm^{-1} , which are
52
53 289 registered for AC, and the intensity decrease of the band at 1018 cm^{-1} . Therefore, from
54
55 290 these results it becomes clear that AC was also oxidized during the preparation of W120
56
57
58
59
60

1
2
3 291 and that reducing structures of AC took part in the oxidation process. Another
4
5 292 absorption band registered for W120 is the weak band at 1643 cm^{-1} that is ascribable to
6
7 293 OH bending of molecular water present in the sample as hydration water of WO_3 . The
8
9 294 broad band at 1114 cm^{-1} denotes contribution to infrared radiation by part of C-O-W
10
11 295 atomic groupings. At frequencies in the range $1000\text{-}600\text{ cm}^{-1}$, absorption may be caused
12
13 296 by $\nu(\text{W}=\text{O})$ and $\nu(\text{W}-\text{O})$ vibrations.^{66,67} Specifically, the characteristic bond vibration
14
15 297 frequency is between 1000 and 948 cm^{-1} for $\text{W}=\text{O}$ and between 870 and 610 cm^{-1} for
16
17 298 $\text{W}-\text{O}$, depending on the WO_3 crystalline phase and its degree of hydration.⁶⁶

20
21
22 299 Comparison of the spectra for S120, T120 and W120 in the regions of around
23
24 300 1720 , 1280 and 1120 cm^{-1} suggests that carboxylic acid groups were formed to a larger
25
26 301 extent for S120 than for W120 and especially for T120 and that correspondingly the
27
28 302 decrease of reducing structures should be also greater for S120. In any event it should
29
30 303 be mentioned here that the relative intensity of the bands at around 1070 and 1020 cm^{-1}
31
32 304 is rather similar for S120 and W120, unlike for T120. In connection with the reactivity
33
34 305 of carbon it was reported before that it is high with oxygen.⁶⁸ However, it was also
35
36 306 found that carbonaceous materials are not oxidized below $175\text{ }^\circ\text{C}$ in air and that the
37
38 307 process is slow even when heating at $250\text{ }^\circ\text{C}$.⁶⁹ Using AC and SnCl_2 , TiO_2 and WO_4^{2-} in
39
40 308 water, reducing structures of AC are oxidized at lower temperatures, especially when
41
42 309 the low-pH SnCl_2 solution is used, which is a relevant finding in relation to the changes
43
44 310 originated in the surface chemistry of AC as a result of the process of preparation of the
45
46 311 AC-MO samples.

47
48
49
50
51 312 **pH of the point zero charge.** As shown in Table 4, the pH_{pzc} is 10.50 for AC, < 1.60
52
53 313 for S120, 9.35 for T120, and 7.90 for W120. The high pH_{pzc} for AC is worth noting as it
54
55 314 is consistent with the presence of chromene and pyrone type basic structures in the
56
57 315 carbon. Evidence for the pyrone-type site as the basic site has been provided before by

1
2
3 316 acid titration and TPD as well as by theoretical calculations.⁷⁰⁻⁷³ Beside the chromene
4
5 317 and pyrone types, the basic behavior of carbon surfaces has been associated with the π
6
7 318 basicity (or Lewis basicity) of the aromatic rings.^{70,74,75} Furthermore, it was stated that
8
9 319 the basicity from the aromatic rings is weak; and the main basicity is still attributed to
10
11 320 the oxygen containing groups.⁷⁶ On the other hand, since chromene and pyrone type
12
13 321 structures not only are reducing in character but also basic in character, their removal
14
15 322 from AC because of oxidation during the preparation of the samples is reflected by the
16
17 323 behavior of the AC-MO samples in acid-base neutralization reactions. Thus, the lower
18
19 324 pH_{pzc} for the AC-MO samples than for AC is in line with a basicity decrease and acidity
20
21 325 increase produced for the AC-MO samples. From the pH_{pzc} values it becomes apparent
22
23 326 that changes originated in surface groups and structures of AC are stronger by the
24
25 327 sequence S120 >> W120 > T120. For the samples, this sequence is in accord with the
26
27 328 extent to which carboxylic acid groups were formed, as shown by the FT-IR analysis of
28
29 329 the samples.
30
31
32
33
34
35
36
37

330

331 ■ CONCLUSIONS

332 The preparation of AC-MO catalysts by wet impregnation of AC with SnCl_2 , TiO_2 and
333 WO_4^{2-} in water at pH 1.37, 5.84 and 9.54, which has been carried out into successive
334 soaking and drying steps, entails marked changes in the surface chemistry of the carbon.
335 By selective oxidation of AC reducing structures, such as chromene and pyrone
336 structures, during the preparation of the samples, $-\text{COOH}$ groups to a larger extent
337 especially with SnO_2 than with WO_3 and TiO_2 are formed. pH_{pzc} is 10.50 for AC, < 1.60
338 for S120, 9.35 for T120 and 7.90 for W120, and therefore the AC-MO samples greatly
339 range in the acid-base character of their surface. With respect to AC, the strongest

1
2
3 340 change in such a character occurs for S120. Obtained results are surely of interest for
4
5 341 preparative, use in catalysis processes, and regeneration purposes of the AC-MO
6
7 342 catalysts.
8
9

10 343
11

12
13
14 344 ■ **AUTHOR INFORMATION**

15
16
17 345 **Corresponding author**

18
19
20 346 *E-mail: vgomez@unex.es
21

22
23 347 **Notes**

24
25
26 348 The authors declare no competing financial interest.
27
28

29 349
30
31

32 350 ■ **ACKNOWLEDGMENTS**

33
34
35
36 351 Financial support from Gobierno de Extremadura and Feder funds (GRU07011,
37
38 352 GRU09122 and GRU10119) is gratefully acknowledged. A. Barroso-Bogeat thanks
39
40 353 Spanish Ministerio de Educación y Cultura for the concession of a FPU grant (AP2010-
41
42 354 2574).
43
44

45 355
46
47

48
49 356 ■ **REFERENCES**

50
51
52 357 (1) Radovic, L. R; Sudhakar, C. Carbon as a Catalyst Support: Production, Properties
53
54 358 and Applications. In *Introduction to Carbon Technologies*; Marsh, H., Heintz, E. A.,
55
56 359 Rodríguez-Reinoso F., Eds.; Universidad de Alicante: Alicante, 1997; pp. 103-165.
57
58
59
60

- 1
2
3 360 (2) Daza, L.; González Ayuso, T.; Mendioroz, S.; Pajares, J. A. Decomposition of
4
5 361 Precursors on Preparation of Rh/Active Carbon Catalysts. *Appl. Catal.* **1985**, 13, 295.
6
7
8 362 (3) Rodríguez-Reinoso, F. Activated Carbon: Structure, Characterization, Preparation
9
10 363 and Applications. In *Introduction to Carbon Technologies*; Marsh, H., Heintz, E. A.,
11
12 364 Rodríguez-Reinoso, F., Eds.; Universidad de Alicante: Alicante, 1997; pp. 35-101.
13
14
15 365 (4) Barroso-Bogeat, A; Fernández-González, C.; Alexandre-Franco, M; Gómez-
16
17 366 Serrano, V. Activated Carbon as a Metal Oxide Support: A Review. In *Activated*
18
19 367 *Carbon: Classifications, Properties and Applications*; Kwiatkowski, J. F., Ed.; Nova
20
21 368 Sci. Pub.: New York, 2011; pp. 297-318.
22
23
24
25 369 (5) Torimoto, T.; Ito, S.; Kuwabata, S.; Yoneyama, H. Effects of Adsorbents used as
26
27 370 Supports for Titanium Dioxide Loading on Photocatalytic Degradation of Propylamide.
28
29 371 *Environ. Sci. Technol.* **1996**, 30, 1275.
30
31
32
33 372 (6) Tao, Y.; Schwartz, S.; Wu, C.-Y.; Mazyck, D. W. Development of a TiO₂/AC
34
35 373 Composite Photocatalyst by Dry Impregnation for the Treatment of Methanol in Humid
36
37 374 Airstreams. *Ind. Eng. Chem. Res.* **2005**, 44, 7366.
38
39
40 375 (7) Tao, Y.; Wu, C.-Y.; Mazyck, D. W. Microwave-Assisted Preparation of
41
42 376 TiO₂/Activated Carbon Composite Photocatalyst for Removal of Methanol in Humid
43
44 377 Air Streams. *Ind. Eng. Chem. Res.* **2006**, 45, 5110.
45
46
47 378 (8) Kubo, M.; Fukuda, H.; Chua, X. J.; Yonemoto, T. Kinetics of Ultrasonic
48
49 379 Degradation of Phenol in the Presence of Composite Particles of Titanium Dioxide and
50
51 380 Activated Carbon. *Ind. Eng. Chem. Res.* **2007**, 46, 699.
52
53
54
55 381 (9) Geng, Q.; Guo, Q.; Cao, C.; Wang, L. Investigation into Nano TiO₂/ACSCR for
56
57 382 Decomposition of Aqueous Hydroquinone. *Ind. Eng. Chem. Res.* **2008**, 47, 2561.
58
59
60

- 1
2
3 383 (10) Wang, X.; Liu, Y.; Hu, Z.; Chen, Y.; Liu, W.; Zhao, G. Degradation of Methyl
4
5 384 Orange by Composite Photocatalysts nano-TiO₂ Immobilized on Activated Carbons of
6
7 385 Different Porosities. *J. Hazard. Mater.* **2009**, 169, 1061.
8
9
10 386 (11) Basha, S.; Keane, D.; Morrissey, A.; Nolan, K.; Oelgemöller, M.; Tobin, J. Studies
11
12 387 on the Adsorption and Kinetics of Photodegradation of Pharmaceutical Compound,
13
14 388 Indomethacin Using Novel Photocatalytic Adsorbents (IPCA). *Ind. Eng. Chem. Res.*
15
16 389 **2010**, 49, 11302.
17
18
19
20 390 (12) Gen, Q.; Cui, W. Adsorption and Photocatalytic Degradation of Reactive Brilliant
21
22 391 Red K-2BP by TiO₂/AC in Bubbling Fluidized Bed Photocatalytic Reactor. *Ind. Eng.*
23
24 392 *Chem. Res.* **2010**, 49, 11321.
25
26
27
28 393 (13) Jamil, T. S.; Ghaly, M. Y.; Fathy, N. A.; Abd el-halim, T. A.; Österlund, L.
29
30 394 Enhancement of TiO₂ Behavior on Photocatalytic Oxidation of MO Dye Using
31
32 395 TiO₂/AC under Visible Irradiation and Sunlight Radiation. *Separ. Purif. Technol.* **2012**,
33
34 396 98, 270.
35
36
37 397 (14) Gao, B.; Yap, P. S.; Lim, T. M.; Lim, T. T. Adsorption-Photocatalytic Degradation
38
39 398 of Acid Red 88 by Supported TiO₂: Effect of Activated Carbon Support and Aqueous
40
41 399 Anions. *Chem. Eng. J.* **2011**, 171, 1098.
42
43
44 400 (15) Slimen, H.; Houas, A.; Nogier, J. P. Elaboration of Stable Anatase TiO₂ through
45
46 401 Activated Carbon Addition with High Photocatalytic Activity under Visible Light. *J.*
47
48 402 *Photochem. Photobiol. A. Chem.* **2011**, 221, 13.
49
50
51
52 403 (16) Huang, D.; Miyamoto, Y.; Matsumoto, T.; Tojo, T.; Fan, T.; Ding, J.; Guo, Q.;
53
54 404 Zhang, D. Preparation and Characterization of High-Surface-Area TiO₂/Activated
55
56 405 Carbon by Low-Temperature Impregnation. *Separ. Purif. Technol.* **2011**, 78, 9.
57
58
59
60

- 1
2
3 406 (17) Asiltürk, M.; Sener, S. TiO₂-Activated Carbon Photocatalysts: Preparation,
4
5 407 Characterization and Photocatalytic Activities. *Chem. Eng. J.* **2012**, 180, 354.
6
7
8 408 (18) Mahadwad, O. K.; Parikh, P. A.; Jasra, R. V.; Patil, C. Photocatalytic Degradation
9
10 409 of Reactive Black-5 Dye Using TiO₂-Impregnated Activated Carbon. *Environ. Technol.*
11
12 410 **2012**, 33, 307.
13
14
15 411 (19) Jo, W.-K.; Won, Y.; Hwang, I.; Tayade, R. J. Enhanced Photocatalytic Degradation
16
17 412 of Aqueous Nitrobenzene Using Graphitic Carbon-TiO₂ Composites. *Ind. Eng. Chem.*
18
19 413 *Res.* **2014**, 53, 3455.
20
21
22
23 414 (20) Sun, J.; Wang, Y.; Sun, R.; Dong, S. Photodegradation of Azo Dye Congo Red
24
25 415 from Aqueous Solution by the WO₃-TiO₂/Activated Carbon (AC) Photocatalyst under
26
27 416 the UV Radiation. *Mater. Chem. Phys.* **2009**, 115, 303.
28
29
30 417 (21) Barroso-Bogeat, A.; Alexandre-Franco, M.; Fernández-González, C.; Gómez-
31
32 418 Serrano, V. FT-IR Analysis of Pyrone and Chromene Structures in Activated Carbon.
33
34 419 *Energy Fuels* **2014**, 28, 4096.
35
36
37
38 420 (22) Barroso-Bogeat, A.; Alexandre-Franco, M.; Fernández-González, C.; Gómez-
39
40 421 Serrano, V. Preparation of Activated Carbon-Metal Oxide Hybrid Catalysts: Textural
41
42 422 Characterization. *Fuel Process. Technol.* **2014**, 126, 95.
43
44
45 423 (23) Barroso-Bogeat, A.; Alexandre-Franco, M.; Fernández-González, C.; Gómez-
46
47 424 Serrano, V. Preparation and Microstructural Characterization of Activated Carbon-
48
49 425 Metal Oxide Hybrid Catalysts: New Insights into Reactions Paths. *J. Mater. Sci.*
50
51 426 *Technol.* **2015**, 31, 806.
52
53
54
55 427 (24) Kahn, A. TiO₂ Coated Activated Carbon for Water Recovery. *J. Undergrad. Res.*
56
57 428 **2002**, 3, June.
58
59
60

- 1
2
3 429 (25) El-Sheikh, A. H.; Newman, A. P.; Al-Daffaee, H.; Phull, S.; Cresswell, N.; York,
4
5 430 S. Deposition of Anatase on the Surface of Activated Carbon. *Surf. Coat. Technol.*
6
7 431 **2004**, 187, 284-292.
8
9
10 432 (26) Ao, Y.; Xu, J., Shen, X., Fu, D., Yuan, C. Magnetically Separable Composite
11
12 433 Photocatalyst with Enhanced Photocatalytic Activity. *J. Hazard. Mater.* **2008**, 160, 295-
13
14 434 300.
15
16
17 435 (27) Newcombe, G.; Hayes, R.; Drikas, M. Granular Activated Carbon: Importance of
18
19 436 Surface Properties in the Adsorption of Naturally Occurring Organics. *Colloids Surf. A*
20
21 437 **1993**, 78, 65.
22
23
24
25 438 (28) Lopez-Ramon, M. V.; Stoeckli, F.; Moreno-Castilla, C.; Carrasco-Marín, F. On the
26
27 439 Characterization of Acidic and Basic Surface Sites on Carbons by Various Techniques.
28
29 440 *Carbon* **1999**, 37, 1215.
30
31
32 441 (29) In *CRC Handbook of Chemistry and Physics*; Lide, D. R., Ed., 2005-2006 86th ed.;
33
34 442 Taylor & Francis: Boca Raton, 2005.
35
36
37 443 (30) Ortiz, A.; Mendoza, M.; Rodríguez Paez, J. E. Naturaleza y Formación de
38
39 444 Complejos Intermedios del Sistema Sn₂Cl₂-NH₄OH-H₂O. *Mater. Res.* **2001**, 4, 265.
40
41
42
43 445 (31) Baes, C. F.; Mesmer, R. E. *The Hydrolysis of Cations*; Wiley: New York, 1976.
44
45
46 446 (32) Cigala, R. M; Crea, F.; De Stefano, C.; Lando, G.; Milea, D.; Sammartano, S. The
47
48 447 Inorganic Speciation of Tin(II) in Aqueous Solution. *Geochim. Cosmochim. Acta* **2012**,
49
50 448 87, 1.
51
52
53 449 (33) Reva, O. V.; Vorob'eva, T. N. Oxidation, Hydrolysis and Colloid Formation in
54
55 450 Storage of SnCl₂ Aqueous Solutions. *Russ. J. Appl. Chem.* **2002**, 75, 700.
56
57
58
59
60

- 1
2
3 451 (34) Remi, R. *Treatise of Inorganic Chemistry*, Vol. 1; Elsevier: Amsterdam, 1956.
4
5
6 452 (35) Séby, F.; Potin-Gautier, M.; Giffaut, E.; Donard, O. F. X. A Critical Review of
7
8 453 Thermodynamic Data for Inorganic Tin Species. *Geochim. Cosmochim. Acta* **2001**, 65,
9
10 454 3041.
11
12
13 455 (36) Huang, W.-F.; Chen, H.-T.; Lin, M. C. The Adsorption and Reactions of SiCl_χ (χ
14
15 = 0-4) on Hydroxylated TiO_2 Anatase (101) Surface: A Computational Study on the
16
17 456 Functionalization of Titania with $\text{Cl}_2\text{Si}(\text{O})\text{O}$ Adsorbate. *Comput. Theor. Chem.* **2012**,
18
19 457 993, 45.
20
21
22
23 459 (37) Fahmi, A.; Minot, C. A. Theoretical Investigation of Water Adsorption on
24
25 460 Titanium Dioxide Surfaces. *Surf. Sci.* **1994**, 304, 343.
26
27
28 461 (38) Freedman, M. J. Polymerization of Anions: The Hydrolysis of Sodium Tungstate
29
30 462 and Sodium Chromate. *J. Am. Chem. Soc.* **1958**, 80, 2072.
31
32
33 463 (39) Przyluski, J.; Kasprzak, M.; Bielinski, J. Investigations of the SnCl_2 -Sensitizing
34
35 464 Solutions for Electroless Plating. *Surf. Coat. Tech.* **1987**, 31, 2003.
36
37
38 465 (40) Davydov, A. A. *Infrared Spectroscopy of Adsorbed Species on the Surface of*
39
40 466 *Transition Metal Oxides*; Wiley: Chichester, 1984.
41
42
43 467 (41) Baraton, M.-I.; Merhari, L. Influence of the Particle Size on the Surface Reactivity
44
45 468 and Gas Sensing Properties of SnO_2 Nanoparticles. *Mater. Trans.* **2001**, 42, 1616.
46
47
48
49 469 (42) Schevchenko, L. L. Infrared Spectra of Salts and Complexes of Carboxylic Acids
50
51 470 and Some of their Derivatives. *Russ. Chem. Rev.* **1963**, 32, 201.
52
53
54 471 (43) Pretsch, E.; Bühlmann, P.; Badertscher, M. *Structure Determination of Organic*
55
56 472 *Compounds. Tables of Spectral Data*; Springer-Verlag: Berlin Heidelberg, 2009.
57
58
59
60

- 1
2
3 473 (44) Kilimov, A. P.; Svechnikova, M. A.; Shevchenko, V. I.; Smirnov, V. V.; Kvasyuk-
4
5 474 Mudryi, F. V.; Zotov, S. B. Infrared Spectra of Cyclic Ethers and their Derivatives.
6
7 475 *Chem. Heterocyclic Compd.* **1967**, 3, 467.
8
9
10 476 (45) Harrison, P. G.; Guest, A. Tin Oxide Surfaces. *J. Chem. Soc., Faraday Trans. 1*
11
12 477 **1987**, 83, 3383.
13
14
15 478 (46) Amalric-Popescu, D.; Bozon-Verduraz, F. Infrared Studies on SnO₂ and Pd/SnO₂.
16
17 479 *Catal. Today* **2001**, 70, 139.
18
19
20 480 (47) Aguilar, C. J.; Ochoa, Y. H.; Rodríguez-Páez, J. E. Obtención de Óxido de Estaño
21
22 481 en el Sistema SnCl₂-H₂O: Mecanismo de Formación de las Partículas. *Rev. Latin Am.*
23
24 482 *Metal. Mat.* **2013**, 33, 100.
25
26
27
28 483 (48) Martos, M.; Morales, J.; Sánchez, L. Mechanochemical Synthesis of Sn_{1-x}M_xO₂
29
30 484 Anode Materials for Li-Ion Batteries. *J. Mater. Chem.* **2002**, 12, 2979.
31
32
33 485 (49) Jiménez, V. M.; Caballero, A.; Fernandez, A.; Espinós, J. P.; Ocaña, M.; González-
34
35 486 Elipe, A. R. Structural Characterization of Partially Amorphous SnO₂ Nanoparticles by
36
37 487 Factor Analysis of XAS and FT-IR Spectra. *Solid State Ionics* **1999**, 116, 117.
38
39
40
41 488 (50) Baraton, M.-I. Fourier Transform Infrared Surface Spectrometry of Nano-Sized
42
43 489 Particles. In *Handbook of Nanostructured Materials and Nanotechnology*; Nalwa, H. S.,
44
45 490 Ed.; Academic Press: San Diego, CA, 1999; pp. 89-93.
46
47
48 491 (51) Haring, R. C.; Walton, J. H. The Autoxidation of Stannous Chloride. II A Survey
49
50 492 of Certain Factors Affecting this Reaction. *J. Phys. Chem.* **1933**, 37, 133.
51
52
53 493 (52) Batzill, M.; Diebold, U. The Surface and Materials Science of Tin Dioxide.
54
55 494 Review. *Prog. Surf. Sci.* **2005**, 79, 47.
56
57
58
59
60

- 1
2
3 495 (53) Mizokawa, Y.; Nakamura, S. ESR Study of Adsorbed Oxygen on Tin Dioxide.
4
5 496 *Oyo Butury* **1977**, 46, 580.
6
7
8 497 (54) Batzill, M. Surface Studies of Gas Sensing Materials: SnO₂. *Sensors* **2010**, 6, 1345.
9
10
11 498 (55) Chang, S. C. Oxygen Chemisorption on Tin Oxide: Correlation between Electrical
12
13 499 Conductivity and EPR Measurements. *J. Vac. Sci. Technol.* **1980**, 17, 366.
14
15
16 500 (56) Bielanski, A.; Haber, J. Oxygen in Catalysis on Transition Metal Oxides. *Catal.*
17
18 501 *Rev. Rev.-Sci. Eng.* **1979**, 19, 1.
19
20
21 502 (57) Teterycz, H.; Klimkiewicz, R.; Laniecki, M. Study of Physico-Chemical Properties
22
23 503 of Tin Dioxide Based Gas Sensitive Materials Used in Condensation Reactions of n-
24
25 504 Butanol. *Appl. Catal. A: Gen.* **2004**, 274, 49.
26
27
28 505 (58) Tanner, R. E.; Liang, Y.; Altman, E. I. Structure and Chemical Reactivity of
29
30 506 Adsorbed Carboxylic Acids on Anatase TiO₂ (001). *Surf. Sci.* **2002**, 506, 251.
31
32
33 507 (59) Zhang, M.; Wu, J.; Lu, D. D.; Yang, J. Enhanced Visible Light Photocatalytic
34
35 508 Activity of TiO₂ Nanotube Array Films by co-Doping with Tungsten and Nitrogen. *Int.*
36
37 509 *J. Photoenergy* **2013**; <http://dx.doi.org/10.1155/2013/471674>.
38
39
40 510 (60) Yates, D. J. C. Infrared Studies of the Surface Hydroxyl Groups on Titanium
41
42 511 Dioxide, and of the Chemisorption of Carbon Monoxide and Carbon Dioxide. *J. Phys.*
43
44 512 *Chem.* **1961**, 65, 746.
45
46
47 513 (61) Primet, M.; Pichat, P.; Pathieu, M.-V. Infrared Study of the Surface of Titanium
48
49 514 Dioxides. II: Acidic and Basic Properties. *J. Phys. Chem.* **1971**, 75, 1221.
50
51
52 515 (62) El-Bahy, Z. M. Adsorption of CO and NO on Ceria- and Pt-Supported TiO₂: In
53
54 516 Situ FTIR Study. *Mod. Res. Catal.* **2013**, 2, 136.
55
56
57
58
59
60

- 1
2
3 517 (63) Vasconcelos, D. C. L.; Costa, V. C.; Nunes, E. H. M.; Sabioni, A. C. S.; Gasparon,
4
5 518 M.; Vasconcelos, W. L. Infrared Spectroscopy of Titania Sol-Gel Coatings on 316L
6
7 519 Stainless Steel. *Mater. Sci. Appl.* **2011**, *2*, 1375.
8
9
10 520 (64) Purans, J.; Kuzmin, A.; Guéry, C. *In-Situ* x-Ray Absorption Fine Structure and x-
11
12 521 Ray Diffraction Studies of Hydrogen Intercalation in Tungsten Oxides. *Proc. SPIE*
13
14 522 **1997**, 2968, 174.
15
16
17
18 523 (65) Emsley, J. *The Elements*; Clarendon Press: London, 1989.
19
20
21 524 (66) Daniel, M. F.; Desbat, B.; Lassegues, J. C.; Gerand, B.; Figlarz, M. Infrared and
22
23 525 Raman Study of WO₃ Tungsten Trioxide and WO₃.xH₂O Tungsten Trioxide Hydrates.
24
25 526 *J. Solid State Chem.* **1987**, *67*, 235.
26
27
28 527 (67) Badilescu, S.; Minh-Ha, N.; Bader, G.; Ashrit, P. V.; Girouard, F. E.; Truong, V.-
29
30 528 V. Structure and Infrared Spectra of Sol-Gel Derived Tungsten Oxide thin Films. *J.*
31
32 529 *Mol. Struct.* **1993**, 297, 393.
33
34
35
36 530 (68) Bansal, R. C.; Goyal, M. *Activated Carbon Adsorption*; CRC Taylor & Francis:
37
38 531 Boca Raton, FL, 2005.
39
40
41 532 (69) Gómez-Serrano, V.; Piriz-Almeida, F.; Durán-Valle, C. J.; Pastor-Villegas, J.
42
43 533 Formation of Oxygen Structures by Air Activation. A Study by FT-IR Spectroscopy.
44
45 534 *Carbon* **1999**, *37*, 1517.
46
47
48 535 (70) Leon y Leon, C. A.; Solar, J. M.; Calemma, V.; Radovic, L. R. Evidence for the
49
50 536 Protonation of Basal Plane Sites on Carbon. *Carbon* **1992**, *30*, 797.
51
52
53
54
55
56
57
58
59
60

- 1
2
3 537 (71) Suárez, D.; Menéndez, J. A.; Fuente, E.; Montes-Morán, M. A. Contribution of
4
5 538 Pyrone-Type Structures to Carbon-Basicity: An ab Initio Study. *Langmuir* **1999**, 15
6
7 539 3897.
8
9
10 540 (72) Suárez, D.; Menéndez, J. A.; Fuente, E.; Montes-Morán, M. A. Pyrone-Like
11
12 541 Structures as Novel Oxygen-Based Organic Superbases. *Angew. Chem. Int. Ed.* **2000**,
13
14 542 39, 1320.
15
16
17 543 (73) Boehm, H. P. Surface Oxides on Carbon and their Analysis: A Critical Assessment.
18
19 544 *Carbon* **2002**, 40, 145.
20
21
22
23 545 (74) Boehm, H. P.; Voll, M. Basische Oberflächenoxide auf Kohlenstoff-I. Adsorption
24
25 546 von Säuren. *Carbon* **1970**, 8, 227.
26
27
28 547 (75) Montes-Morán, M. A.; Menéndez, J. A.; Fuente, E.; Suárez, D. Contribution of the
29
30 548 Basal Planes to Carbon Basicity: An ab-Initio Study of the H₂O⁺- π Interactions in
31
32 549 Cluster Models. *J. Phys. Chem. B* **1998**, 102, 5995.
33
34
35
36 550 (76) Yang, R. T. *Adsorbents: Fundamentals and Applications*; Wiley: Hoboken, 2003.
37
38
39 551
40
41
42 552
43
44
45
46
47
48
49
50
51
52
53
54
55
56
57
58
59
60

553

Table headings554 **Table 1. Preparation of the Samples**555 **Table 2. Elemental Analysis of AC and AC-MO Samples**556 **Table 3. FT-IR Spectrum of AC. Position and Assignment of Bands**557 **Table 4. pH_{pzc} Measured for AC and AC-MO Samples**

558

559

560

561

Caption to figures562 **Figure 1.** FT-IR spectra of AC, S120, T120 and W120 between 4000 and 2000 cm^{-1} .563 **Figure 2.** FT-IR spectra of AC, S120, T120 and W120 between 2000 and 400 cm^{-1} .564 **Figure 3.** FT-IR spectrum of TiO_2 (anatase powder) between 2000 and 400 cm^{-1} .565 **Figure 4.** Expanded FT-IR spectrum between 2000 and 400 cm^{-1} for W120.

566

567

568

569

570 **Table 1**

precursor	pH	yield (wt%)	codes
SnCl ₂ ·2H ₂ O	1.37	149	S120
TiO ₂ anatase	5.84	103	T120
Na ₂ WO ₄ ·2H ₂ O	9.54	106	W120

571

572

573 **Table 2**

sample	C (wt%)	H (wt%)	N (wt%)	S (wt%)	O _{diff.} (wt%)
AC	86.50	0.51	0.26	0.64	12.09
S120	52.32	1.25	0.06	0.37	46.00
T120	85.81	0.20	0.55	0.63	12.81
W120	78.32	0.98	0.20	0.61	19.89

574

575

576 **Table 3**

spectral feature	position (cm ⁻¹)	Assignment	group / structure
Peaks	2972-2823	<i>v</i> (C-H) <i>v</i> (O-H)	chromene structures quinone oximes
Band	1720	<i>v</i> (C=O)	carboxylic acid group, 2-pyrone structure
shoulder	1657	<i>v</i> (C=O)	pyrone and chromene structures, carbonyl structures
shoulder	1636	<i>v</i> (C=C)	pyrone and chromene structures
Band	1566	<i>v</i> _s (C=C) skeletal	aromatic ring
		<i>v</i> (C=C)	2-pyrone structures
Band	1279	δ (O-H)- <i>v</i> (C-O)	carboxylic acid
		<i>v</i> _{as} (=C-O-C)	4H-chromene
shoulders	ca. 1249	<i>v</i> _{as} (=C-O-C)	2H-chromene, 2-pyrone
band	1024	<i>v</i> _s (=C-O-C)	chromene, pyrone and ether structures

Abbreviations: *v*, stretching; δ , bending (in-plane); as, asymmetric; s, symmetric.

577

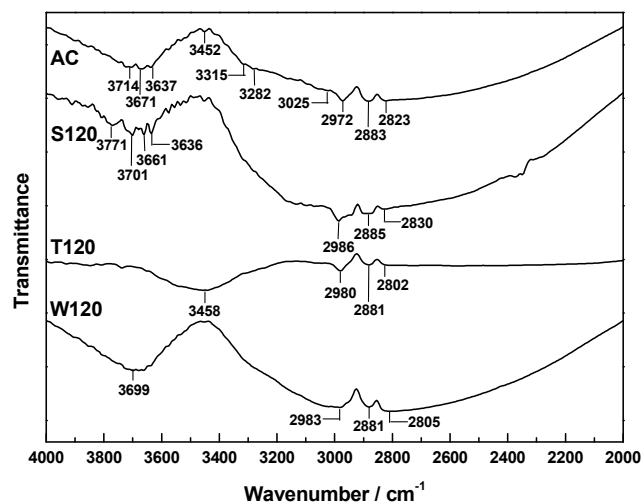
578

1
2
3 579
4
5
6 580 **Table 4**
7
8

<u>sample</u>	<u>pH_{pzc}</u>
AC	10.50
S120	< 1.60
T120	9.35
W120	7.90

9
10
11
12
13
14
15 581
16
17
18 582
19
20
21
22
23
24
25
26
27
28
29
30
31
32
33
34
35
36
37
38
39
40
41
42
43
44
45
46
47
48
49
50
51
52
53
54
55
56
57
58
59
60

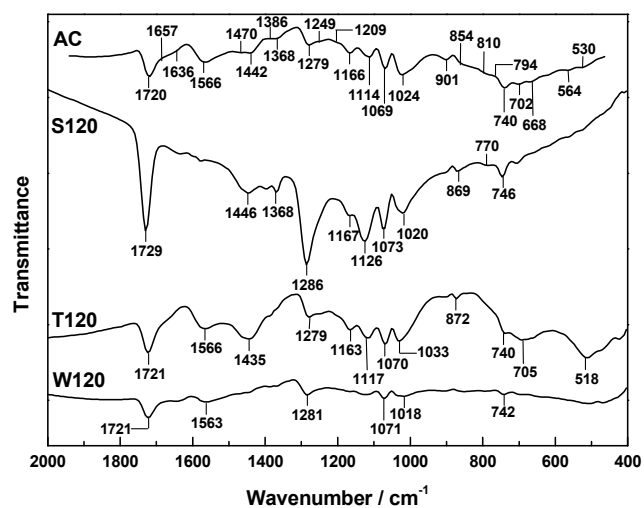
583 Fig. 1



584

585

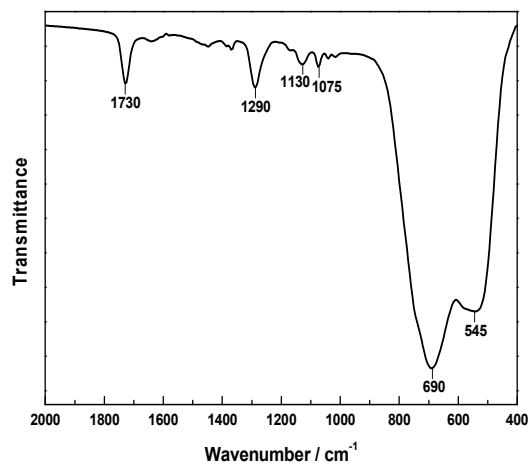
586 Fig. 2



587

588

589 Fig. 3

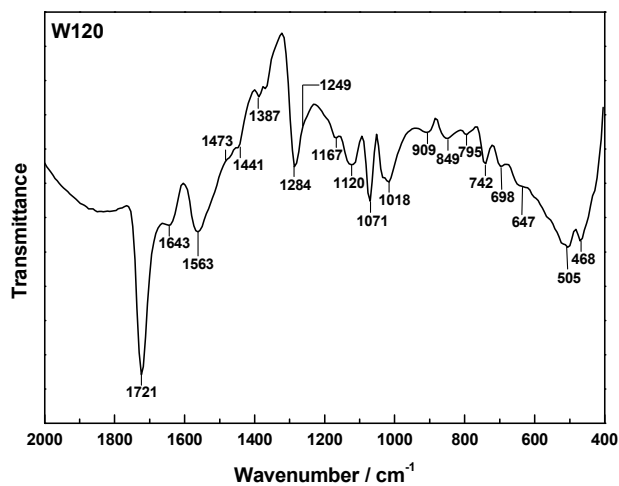


590

591

592

593 Fig. 4



594

595

596 TOC

597

